Nirma Univ J Pharm Sci; 2021, 8(1&2) 17-36

ISSN 2348 –4012

ARTICLE

IDENTIFICATION OF NOVEL SARS-COV-2 ENTRY INHIBITORS VIA STRUCTURE BASED HIERARCHICAL VIRTUAL

Shivani Patel[1], Palmi Modi[2], P. K. Patel[3], Vivek K. Vyas[1*]

[1]Department of Pharmaceutical Chemistry, Institute of Pharmacy, Nirma University, Ahmedabad, 382481, Gujarat, India.

[2]L J Institute of Pharmacy, Ahmedabad 382210, Gujarat, India

[3]Department of Chemistry, M. G. Science Institute, Navarangpura, Ahmedabad 380009, Gujarat, India

**Corresponding author:*

Dr. Vivek K. Vyas

E-mail: vivekvyas@nirmauni.ac.in

ABSTRACT

A novel coronavirus (2019-nCov) is a pneumatic infectious disease caused by severe acute respiratory syndrome coronavirus 2 (SARS-CoV-2) has declared pandemic by the World Health Organization (WHO). However, there is no efficient drug therapy available to combat with this deadliest disease. By considering the public-health emergency, most of the SARS-CoV inhibitors and antiviral drugs are utilized for the treatment of COVID-19 infection. Herein, we presented integrated drug design strategies using E-pharmacophore modeling, molecular docking and molecular dynamic simulation studies based on the recently published SARS-CoV-2 RBD protein structure. Structure-based pharmacophore model (ADHRR) and high-throughput virtual screening (HTVS) were used to screen ZINC and ChEMBL molecular databases for identifying novel SARS-CoV-2 entry inhibitors. The retrieved potential hits were taken for the comparative molecular docking against SARS-CoV-2 and SARS-CoV enzymes to understand the different binding interactions. Further, the stability of receptor-ligand complex and specific amino acid interactions was evaluated by performing molecular dynamic simulation of 30 ns in solvated model system. This study

identified ZINC00662497, ZINC00669387, ZINC08426008, ZINC0660155 and ZINC0844005 as promising leads for inhibiting the entry of 2019-nCoV virus.

Keywords: *Corona virus, E-pharmacophore modelling, Molecular docking, Molecular dynamic simulation, SARS-CoV-2 entry inhibitors*

INTRODUCTION

Several members of corona viridae family are constantly circulating in human population and causing acute/ mild respiratory diseases. The mild and asymptomatic infections are caused by alpha-coronavirus, whereas severe acute respiratory syndrome coronavirus (SARS-CoV) and Middle East respiratory syndrome coronavirus (MERS-CoV) are beta-coronaviruses caused serious epidemics [1]. Severe acute respiratory syndrome coronavirus (SARS-CoV) and Middle East respiratory syndrome coronavirus (MERS-CoV) are transmitted from animals to humans. The SARS emerged in 2002 from horse shoe and bats, natural reservoir hosts for SARS-CoV [2]. Human transmission was facilitated by intermediate hosts like civet cats and raccoon dogs [3]. In 2012, it recurrence in the form of MERS-CoV; HCoV-229E, HCoV-OC43, HCoVNL63 and HCoV-HKU1 are few other coronaviruses responsible for human infections [4]. The re-emergence of coronavirus (2019-nCoV), officially named as SARS-coronavirus 2 (SARS-CoV-2) has created alarming situation and demanding potential therapeutic to preclude the death of infected patients [5]. However, there is no approved drug therapy is available for the treatment of COVID-19 disease. Recent treatments are focused on quarantine and containment of infected patient to minimize the human transmission [6]. The cellular entries of coronaviruses facilitate by viral surface spike protein (S-protein). Their attachment depends on the interactions between envelope-anchored spike glycoprotein (SARS) and angiotensin-converting enzyme 2 (ACE2) receptor on the surface of target cells [7]. The S-protein is homotrimeric in which each monomer comprised of two subunits, S1 contains receptor binding domain (RBD) and S2 implicates viral fusion on cell membrane [8]. Sequence similarity between SARS-CoV and SARS-CoV-2 spike protein is about 80% [9]. Moreover, amino acid residues S-RBD of SARS-CoV-2 are highly conserved with S-RBD of SARS-CoV of bats, human, and civet. The binding affinity of S-RBD of SARS-CoV-2 and ACE2 is approximately ten times higher than SARS-CoV RBD, indicating that ACE2 is the specific receptor responsible for the SARS binding to the host cell [10]. Thus, virus specific molecular interaction of SARS-S/ACE2 proteins is considered as a promising therapeutic target for discovery of newer SARS-CoV-2 entry inhibitors. Furthermore, many research reports are available for targeting viral entry

inhibitors, such as hydroxychloroquine [11], camostat [12], umifenovir [13], etc for minimizing the COVID-19 infection. Discovery of newer entry inhibitors can be considered as potential cure for minimizing the exponentially expending of COVID-19 infection [14]. Molecular modelling methods such as structure-based pharmacophore mapping is a useful tool in order to describe structural and functional requirements of the molecules for biological activity. Pharmacophore model when search against molecular data base as a 3D search query retrieves molecules, which possess almost similar features as per the requirement to achieve desired biological activity [15,16] . Herein, we used receptor structure-based E-pharmacophore model for database screening, followed by high-throughput virtual screening using recently published receptor-binding domain (S-RBD) of SARS-CoV-2. Firstly, the database comprised of molecules from ZINC and ChEMBL libraries was screened by receptor-based energy-optimized pharmacophore model. Further, the identified hits comprising of essential pharmacophoric features were considered for molecular docking based high-throughput virtual screening to recognize their essential binding interactions and binding affinities. Finally, the most promising retrieved hits were taken for comparative docking study against both SARS-CoV and SARS-CoV-2 RBD proteins to gain the different binding insights. The essential residual interactions were validated and dynamic behaviour of protein-ligand complex was determined by performing the molecular dynamic simulation for 30 ns. These identified leads may be developed as potential antiviral agents for preventing the spread COVID-19 infections (Fig.1).

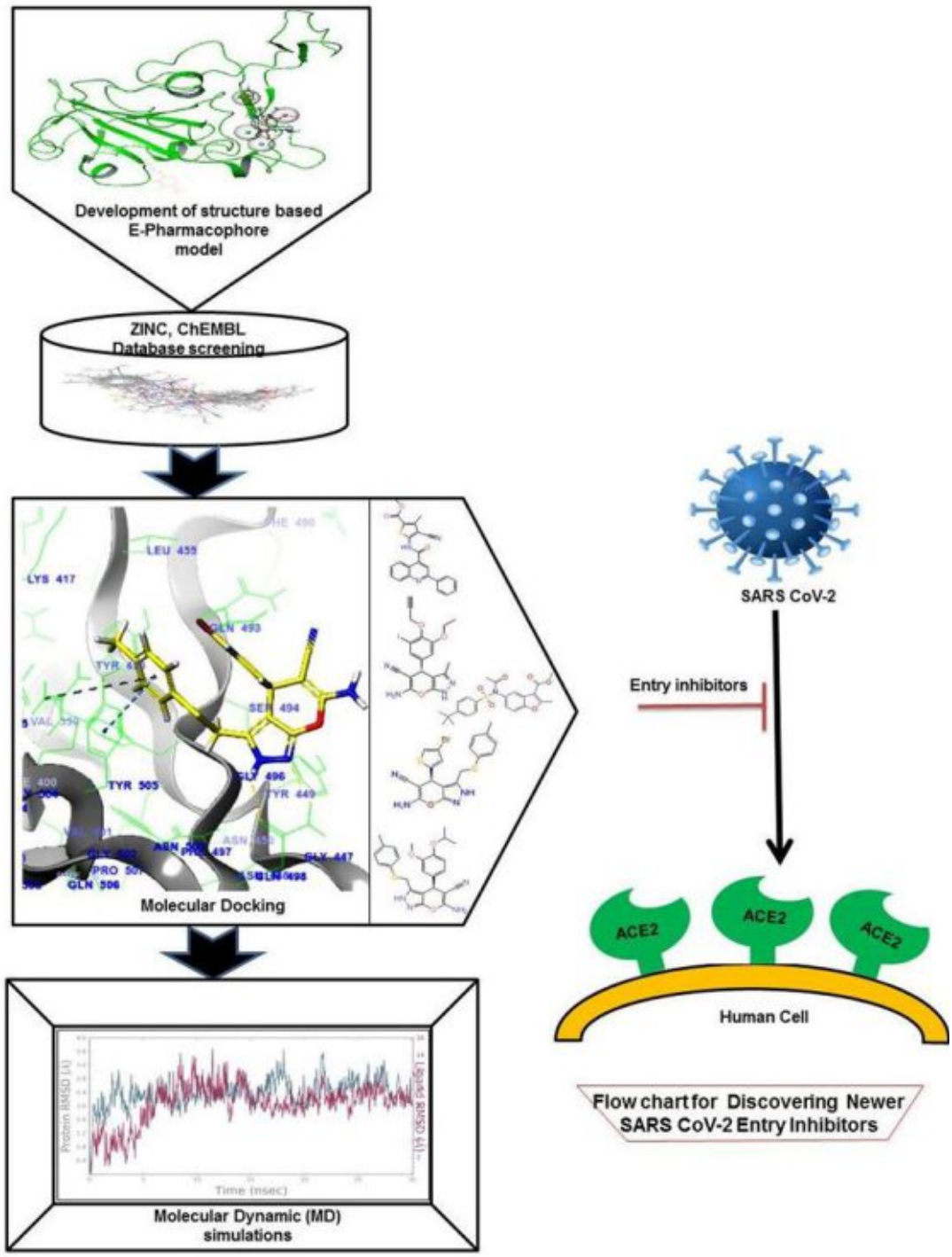

Figure 1. Overall Study Workflow.

MATERIALS AND METHODS

Protein preparation and receptor grid generation

The crystal structure of SARS-CoV and SARS-CoV-2(COVID-19) spike receptor-binding domain proteins (PDB ID: 6M0J, 2AJF) complexed with human ACE-2 was downloaded from Protein Data Bank [17,18]. The proteins were prepared by assigning bond orders, adding H- atoms and removing water molecules using Protein preparation Wizard (Maestro, v11.4, Schrödinger, LLC, NewYork, NY, USA). The atom types were assigned and charge state was optimized. Finally, the structures were minimized by OPLS-2005 force field by converging the heavy atoms to RMSD of 0.3 Å. As, there was no co-crystalized ligand available in the protein structure, 20 × 20 × 20 Å grid was generated by selecting amino acid residues (Lys 417, Tyr 449, Tyr 453, Phe 486, Asn 487, Gln 493, Gly 496, Gln 498, Thr 500, Asn 501, Gly 502 and Tyr 505) [9] using Receptor Grid Generation module (Maestro, v11.4, Schrödinger, LLC, New York, NY, USA).

Molecular database construction and ligand preparation

We performed virtual screening against two molecular databases for the identification of novel entry inhibitors. ZINC [19] includes 2500 molecules and ChEMBL [20] includes 160 molecules. Both the libraries were screened using refined 3D search query for drug like properties, such as molecular weight (150-500); xlogP (-4to5); rotatable bond (8); polar surface area (150); hydrogen-bond donar (10); hydrogen-bond acceptor (10). The database was constructed by merging both molecular libraries followed by ligand preparation and ADMET filtration using phase module. Ligand preparation involved addition of hydrogen atoms, removal of salt, and generation of stereoisomers, ionization at pH (7 ± 2) and determining valid 3D conformation. All the compounds were filtered based on their drug-like properties.

Protein sequence similarity

The SARS-CoV and SARS-CoV-2 (COVID-19) spike proteins and their sequences were downloaded from the protein data bank (PDB). The sequence similarity was assessed by superimposing Chain E of proteins using protein sequence similarity tool of Schrödinger software.

E-pharmacophore generation and validation

Three promising entry inhibitors were docked against previously prepared receptor grid of SARS-CoV-2 protein using glide module. Energy-optimized structure-based pharmacophore (E-pharmacophore) was built by retrieving glide XP descriptors information and mapping the energy terms on the atoms [21]. E-pharmacophore was built by mapping the Glide XP energies for the best

docked complex using phase module (Schrödinger, LLC, NY, USA, 2017). The pharmacophore hypothesis ADHRR was generated based on the identified pharmacophoric features of hydrogen bond acceptor (A); hydrogen bond donor (D); hydrophobic (H) and ring aromatic (R) using develop pharmacophore from receptor-ligand complex' option in Phase module. The performance of pharmacophore hypothesis was evaluated by calculating Enrichment Factor (EF) calculation. For that, 20 actives and dataset of 1000 decoys was downloaded from Schrödinger (http://www.schrodinger.com /glidedecoyset) [22]. The enrichment factor at 1% indicated the enhanced recovery of known actives over the decoys. Boltzmann-enhanced discrimination of receiver operating characteristic curve (ROC) i.e., BEDROC (α=20.0) metrics exhibits enhanced recognition of known actives over decoys from the internal database [23].

E-pharmacophore database screening

A five-point pharmacophore model ADHRR was used to screen molecular database containing 2660 compounds. The database screening was performed by adjusting minimum features match of 4 out of 5 sites in ligand and one inter site distance constrain in Phase module [24,25]. Screening was processed by generating conformers for each ligand, matching the excluded volumes and inter site distance tolerance was set at 2.0 Å. The screened compounds were ranked based on their fitness score, alignment score, volume and RMSD value. The compounds with the best fitness score were subsequently subjected for high throughput virtual screening. The HTVS docking is quick and more tolerant to suboptimal fits than standard precision (SP) and extra precision (XP) docking study [26]. For docking study, ligands were prepared, filtered based on their drug like properties and receptor grid was defined by selecting the reported amino acid residues. Compounds with the best docking score and glide score were subjected to XP docking.

Comparative molecular docking studies

The retrieved compounds from HTVS screening were taken for the rigid XP (extra precision) docking against 6M0J and 2AJF proteins [27]. The shape and properties of receptors were represented by computing a grid box by selecting protein residues using receptor grid generation panel. Ligands were prepared and chemical correctness was achieved by protonation, ionization variations, energy minimization and tautomerization at pH 7.0 using Ligprep module. Comparative docking study was performed using XP docking algorithm in glide module by keeping van der Waals scaling factor at 1.0. Further, the protein-ligand interactions were identified and docking poses were visualized by Maestro interface 11.4. The best docked ligand with the highest XP score was

considered for molecular dynamic simulation study.

In silico ADMET prediction

The ADMET properties of retrieved hits, mainly partition coefficient (QPlogPo/w), water solubility (QPlogS), cell permeability, (QPPCaco-2), % human oral absorption and HERG K^+ IC_{50} (QPlogHERG) were predicted using the QikProp module. It predicted 44 physicochemical and pharmacokinetic descriptors values based on 95% of known drugs in the normal mode with default setting [28].

Molecular dynamics simulations

A molecular dynamic simulation (MD) of SARS-CoV-2-ZINC00662497 complex was performed using Desmond module (Schrödinger, LLC, NY, USA, 2017). For that, protein-lead complex was inserted in to SPC water model and minimized using OPLS-2005 force field [36]. The three-step process included system builder, minimization and molecular dynamics. A system was built on the receptor using SPC system builder having 10 Å buffered orthorhombic boundary box. The system was solvated using TIP3P water molecules and neutralized using 0.15M NaCl [22]. The energy of neutralized system was minimized by steepest descent method having maximum 2000 steps with or without solute restrains. Particle mesh Ewald (PME) method was used to calculate long range electrostatic interactions and van der Waals and short-range electrostatic interactions were truncated at 9.0. The SHAKE algorithm was applied for limiting the movements of hydrogen atoms of covalent bonds. Nose–Hoover thermostats were utilized to maintain constant simulation temperature, and Martina–Tobias–Klein method was used to control pressure throughout simulation. The simulation was carried out at 300 K and 1.0 bar pressure using Berendsen thermostat and barostat [29]. The system was relaxed for 2 ns before productive simulation of 30 ns having recorded trajectory at time interval of 5.0 ns. The intermolecular hydrogen bond interactions, energy potential and root mean square deviation (RMSD) were examined to exhibit stability of receptor-ligand complex.

RESULTS AND DISCUSSION

Generation of E-pharmacophore model

As, there is no co-crystalized ligand available in SARS-CoV-2 protein structure; the residual based receptor grid was generated by performing docking of known antiviral entry inhibitors (umifenovir, camostat and hydroxychloroquine) into the identified binding site and represented in Fig. 2. The various receptor-ligand complexes were evaluated based on their binding interactions and docking poses.

Further, the best dock complex was considered to generate energy-optimized

pharmacophore model using development of common pharmacophore hypothesis option available in phase module. The E-pharmacophore model was developed by mapping Glide XP energetic terms on the pharmacophoric sites, which were evaluated from structural and energy information of protein-ligand complex. We developed five-point pharmacophore hypothesis ADHRR comprised of one hydrogen bond acceptor, one hydrogen bond donor, one hydrophobic and two ring aromatic features. The structure-based pharmacophore model was generated in such way, that it could effectively map all the structural features, which are responsible for biological activity.

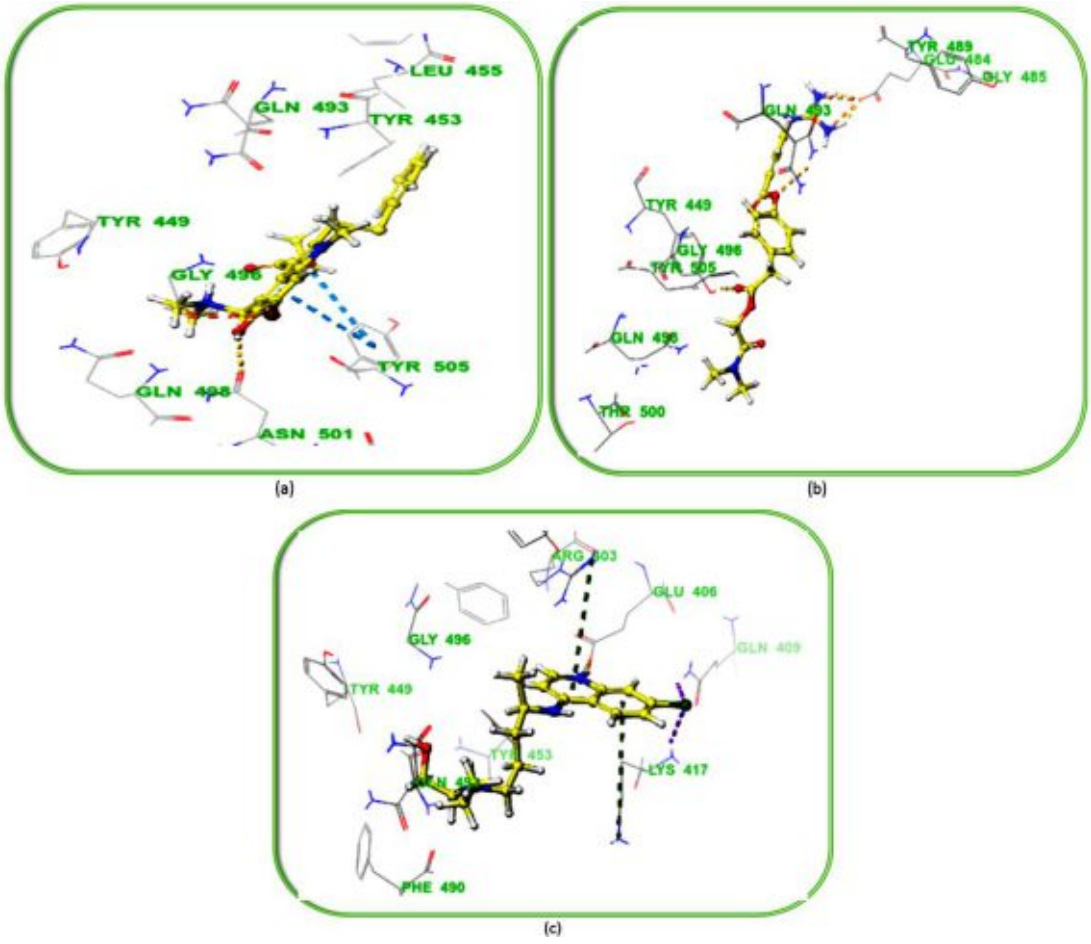

Figure 2. Residual interactions of a) Umifenovir; b) Camostat and c) Hydroxychloroquine at the binding site of SARS CoV-2 RBD (PDB ID: 6M0J)

Validation of energy-optimized pharmacophore

The performance of generated E-pharmacophore model was evaluated by screening the molecular library using validation of pharmacophore hypothesis module in Phase. The internal molecular library composed of 20 known actives obtained from literature and 1000 decoy molecules downloaded from Schrödinger. After screening statistical parameters, mainly total hits (H_t); % ratio of actives; % yield of actives; model enrichment factor (EF); false negative; false positives; goodness of hit score (GH), N% of sample size and BEDROC (α=20) were calculated (Table 1).

Table 1: Goodness-of-hit (GH) Scoring Parameters of ADHRR

Serial No.	Parameter	Values
1	Total number of decoy molecules (D)	1000
2	Total number of Active molecules (A)	20
3	Total hits (Ht)	26
4	Active hits (Ha)	18
5	% Yield of Actives [(Ha/Ht)X100]	70
6	% Ratio of Actives [(Ha/A)X100]	90
7	Enrichment factor (EF)*	34.61
8	False positives, FP [Ht-Ha]	08
9	False negatives, FN [A-Ha]	02
10	Goodness of hit (GH)*	0.72

EF= [(Ha X D)/(Ht X A)]; GH= [$Ha(3A+H_t)/(4H_tA)$]*[1-[H_t-H_a)/(D-A)]

The enrichment factor matrices measure the actives in the top ordered list compared to decoys from the internal library. Further, the GH score ranges from 0 to 1, where 0 exhibits the null model and 1 represents the ideal model. The receiver operative characteristic curve (ROC) metric represents the linearly scaled average of actives positions and ranked within the library. The ROC is ranging from 0 to 1; Truchon and Bayly suggested ROC e" 0.7 as a desirable performance value.

BEDROC denotes the early identification of actives from the database ranging from 0-1 in which α=20.0 exhibits 80% of the BEDROC results come from the first 8% of ranked molecules. The EF (34.61), ROC (0.93), AUC (0.95), RIE (14.69) and BEDROC (α=20) (0.939) indicated efficiency of generated pharmacophore hypotheses to identify actives from the ranked molecules in the internal library (Table 2). Finally, this statistically significant five features E-pharmacophore hypothesis was considered for the database screening.

Table 2: Enrichment Matrices for Energy-Optimized Pharmacophore (ADHRR) Validation

Serial No.	PARAMETERS	VALUES
1	ROC	0.93
2	AUC	0.95
3	RIE	14.69
4	EF	34.61
5	BEDROC(α=8)	0.923
6	BEDROC(α=20)	0.939
7	BEDROC(α=160)	0.980

ROC= receiver operating characteristic; AUC = Area under curve; RIE = Robust initial enhancement; EF = enrichment factor; BEDROC = Boltzmann-enhanced discrimination of receiver operating characteristic.

Database screening

The validated E-pharmacophore hypothesis (ADHRR) was employed to screen the constructed database containing 2500 molecules from ZINC and 160 molecules from ChEMBL library using database screening option in Phase module. The database was screen by matching maximum number of features is 4 out of 5 and applying one inter site distance constrain. E-pharmacophore based screening identified 350 molecules based on their highest fitness and alignment score from the database. The retrieved molecules were further filtered by hierarchical structure based molecular docking protocol of high throughput virtual screening (HTVS) in Glide module. These hits were pre-filtered by calculating ADMET

properties within the module. Subsequently, they were subjected for the Glide HTVS/SP/XP docking in the designated binding site of SARS-CoV-2 protein (PDB ID: 6M0J). Total 250 compounds were obtained from HTVS; 158 compounds resulted from SP and 135 compounds retrieved from XP docking studies. Finally, the resulted hits with better Glide XP score and docking pose were analysed.

Comparative docking analysis

The retrieved hits from high throughput virtual screening having SP docking score e" -7.0 kcal/mol were subjected for the comparative molecular docking analysis against SARS CoV-2 and SARS CoV. The extra precision (XP) rigid docking was performed in the constraint grid of 6M0J and 2AJF proteins to analyse the different binding interactions. Total 75 hits were docked into the active site of receptor binding domains of SARS CoV-2 and SARS CoV.

Top15 virtual hits with their fitness score, glide score and XP scores are summarized in Table 3.

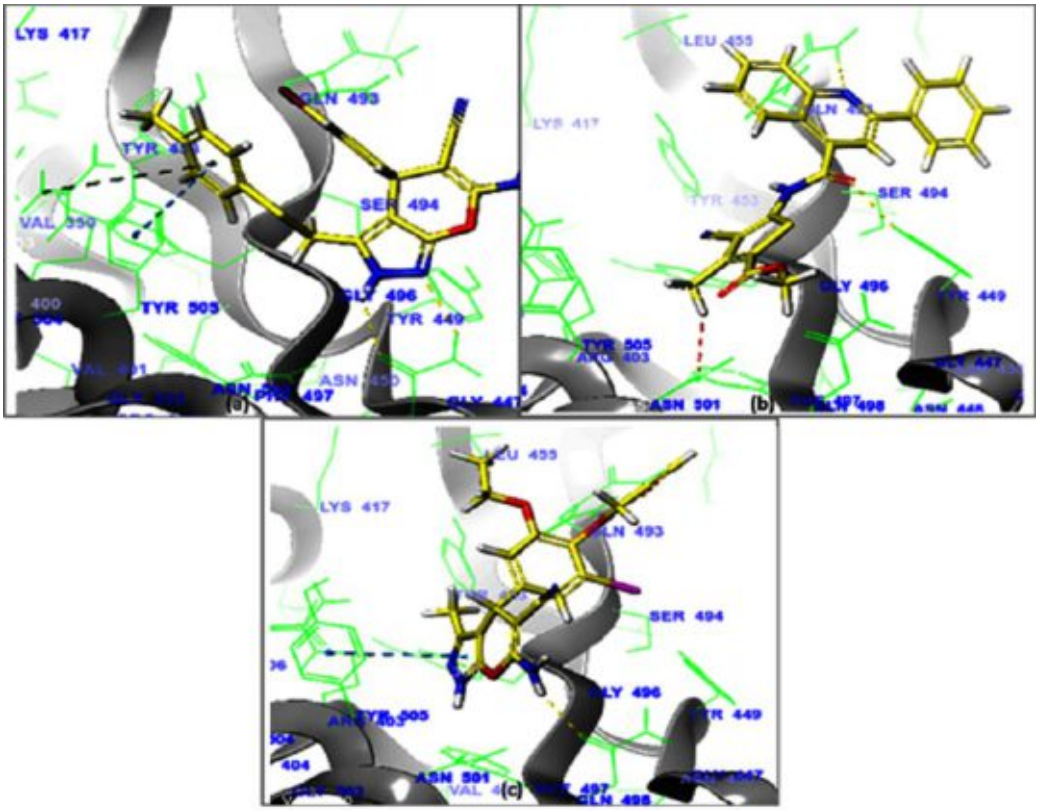

Figure 3. Residual Interactions of a) ZINC00662497, b) ZINC00669387 and c) ZINC08426008 at the Binding Site of SARS-CoV-2 (PDB: 6M0J)

The greater binding affinities for SARS-CoV-2 was identified by the higher docking score of -8 to -7 kcal/mol, whereas the lowest docking score of -6 to -3 kcal/mol indicated less binding affinity for SARS–CoV. The best docked compounds were ZINC00662497, ZINC00669387, and ZINC08426008 against the both the proteins are presented in the Figure 3 and 4. ZINC00662497 has docking score of -8.197 kcal/mol at the binding site of 6M0J protein; the amino group of 2,4-dihydropyrano pyrazole formed H-bonding with Gly 496 and Tyr 449; phenyl ring exhibited pi–pi stacking with Tyr 505 and formed hydrophobic contacts with Val 350.

Table 3: Top 15 Virtual Hits with Their Highest Fitness Score and Binding Free Energy to SARS- Cov-2 and SARS-Cov Enzymes.

Sr No.	Compound Name	Fitness Score	SARS CoV-2		SARS CoV	
			glide gscore	XP GScore (kcal/mol)	glide gscore	XP GScore (kcal/mol)
1	ZINC00662497	1.754	-8.197	-8.197	-5.832	-5.836
2	ZINC00669387	1.577	-8.101	-8.101	-5.539	-5.539
3	ZINC08426008	1.733	-8.057	-8.057	-5.457	-5.457
4	ZINC0660155	1.749	-7.975	-7.975	-5.765	-5.775
5	ZINC0844005	1.624	-7.924	-7.924	-5.289	-5.289
6	ZINC00688318	1.638	-7.870	-7.875	-6.095	-6.095
7	ZINC00688321	1.571	-7.844	-7.844	-4.857	-4.857
8	ZINC02497152	1.553	-7.785	-7.788	-3.933	-3.933
9	ZINC10009832	1.476	-7.698	-7.698	-3.457	-3.457
10	ZINC02170042	1.442	-7.671	-7.671	-3.539	-3.539
11	ZINC02497224	1.429	-7.503	-7.505	-3.766	-3.764
12	ZINC08426766	1.377	-7.415	-7.415	-4.888	-4.888
13	38	1.418	-7.371	-7.371	-3.325	-3.325
14	13	1.315	-7.351	-7.351	3.623	-3.623
15	55	1.626	-7.258	-7.258	-3.317	-3.317

ZINC00669387 possessed docking score of -8.101 kcal/mol; the nitrogen of quinoline ring formed H-bonding interaction with Gln 493 and amidic oxygen formed H-bonding with Tyr 449; 3-CH_3 group of 5-amino-4-cyano-3-methylthiophene ring showed hydrophobic contacts with Asn 501 of SARS –CoV-2 protein. The binding affinity of ZINC08426008 for SARS–CoV-2 spike glycoprotein was demonstrated by docking score of -8.057 kcal/mol; 6-NH_2 group of 6-amino-3-methyl-1,4-dihydropyrano pyrazole ring formed H-bonds with Gly 496 and 2-propylnyoxy substituent of 1-ethoxy-3-iodo-2-(propynyloxy)phenyl ring also exhibited H-bonding interaction with Gly 493; pi–pi interactions were observed between 1,4-dihydropyrano pyrazole and Tyr 505. Residues Tyr 449, Gln 493, Gly 496, Asn 501 and Tyr 505 are the most prominent for the binding interactions in SARS-CoV-2 protein (Figure 3).

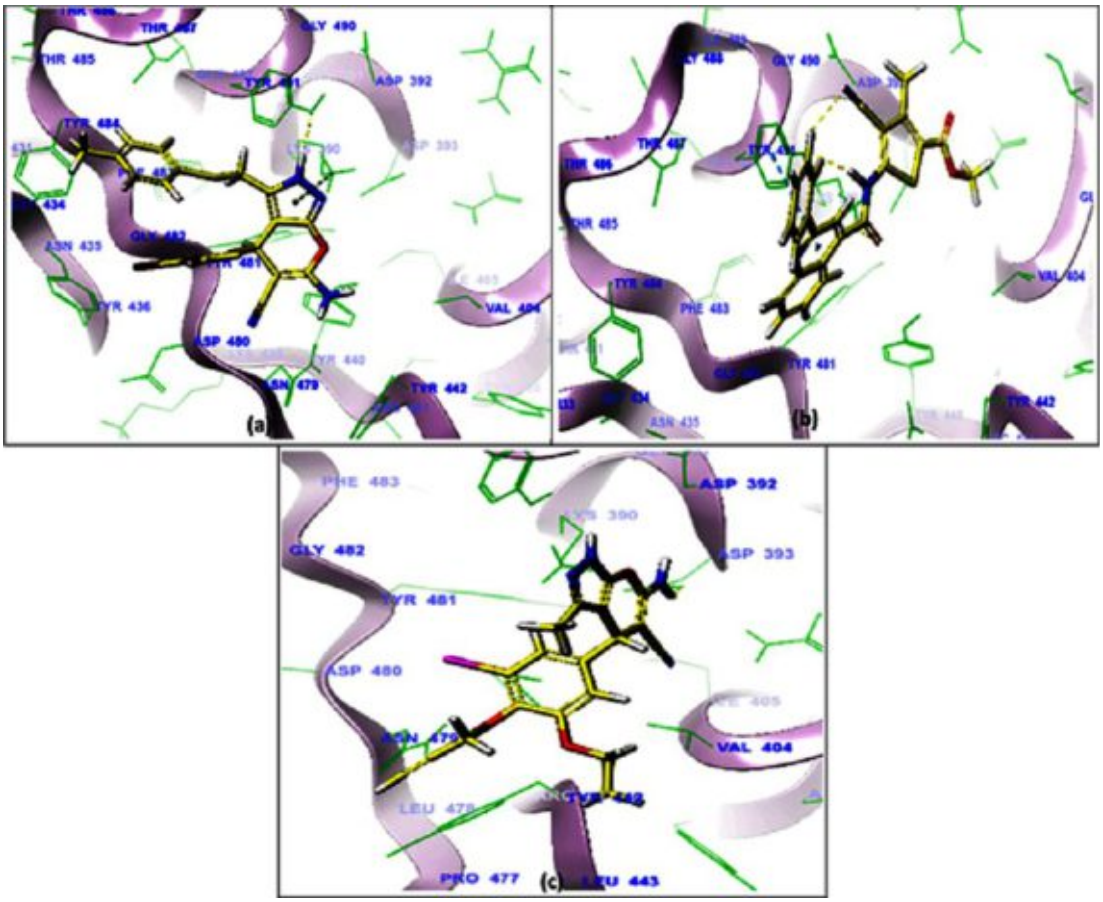

Figure 4. Residual Interactions of a) ZINC00662497, b) ZINC00669387 and c) ZINC08426008 at the Binding Site of SARS-CoV-1(PDB: 2AJF).

In comparative docking study ZINC00662497 exhibited the lowest binding energy of -5.836 kcal/mol at the binding site of SARS-CoV protein. The 2, 4-dihydropyrano pyrazole formed H-bonding interaction with Tyr 491 and hydrophobic contacts with Lys 390. The ZINC00669387 represented minimum docking score of -5.539 kcal/mol against 2AJF protein; -NH of amide bond and 5–NH_2 of 5-amino-4-cyano-3-methylthiophene showed H-bonding interactions with Tyr 491; pi-pi stacking was observed between the phenyl ring and Tyr 491. Further, ZINC08426008 exhibited relatively less binding affinity of -5.457 kcal/mol for SARS-CoV protein; 6-NH_2 group of 6-amino-3-methyl-1, 4-dihydropyrano pyrazole ring formed H-bond with Asp 393. As shown in the Figure 4 residues, Lys 390, Asp 393 and Tyr 491 are important for interactions at the active site of SARS-CoV. Overall, the highest binding energy indicated that identified leads showed good binding affinities for SARS-CoV-2 compared to SARS-CoV protein.

Molecular dynamics (MD) simulation

The best docked 6M0J- ZINC00662497 complex was subjected to MD simulation to gain the dynamic comprehension of binding interactions for time period of 30ns. The stability of protein-ligand complex was studied by analysing RMSD and RMSF plots of protein backbone compared to its initial frame structure. The protein trajectory fluctuated between the RMSD of 2.4 Å to 3.6 Å as displayed in Fig. 5a. The ligand RMSD between 1.2 Å to 3.0 Å indicated the stability of ligand within binding pocket of protein during the simulation. The difference between the RMSD values of ligand and protein reflected the stability of ligand throughout the simulation. Further, the RMSF analysis of protein backbone exhibited fluctuation of N- and C-terminal residues as shown in Fig.5b. Most of the protein residues fluctuate below 2.0 Å and larger fluctuation up to 5.0 Å. As shown in the Fig. 5c the RMSF value of ligand was also about 2.5 Å. The favourable amino acid interactions with ligand atoms were also analysed. Residues Lys 417, Tyr 449, Asn 487, Gln 493, Gly 496, Gln 498, Asn 501 and Gly 502 formed hydrogen bonding interactions during the simulation. The Lys 417 also exhibited water bridges and ionic interactions with the inhibitors. Tyr 449, Phe 486, Thr 500 and Tyr 505 displayed hydrophobic contacts and Pi-Pi interactions with ZINC00662497 (Fig. 5d).

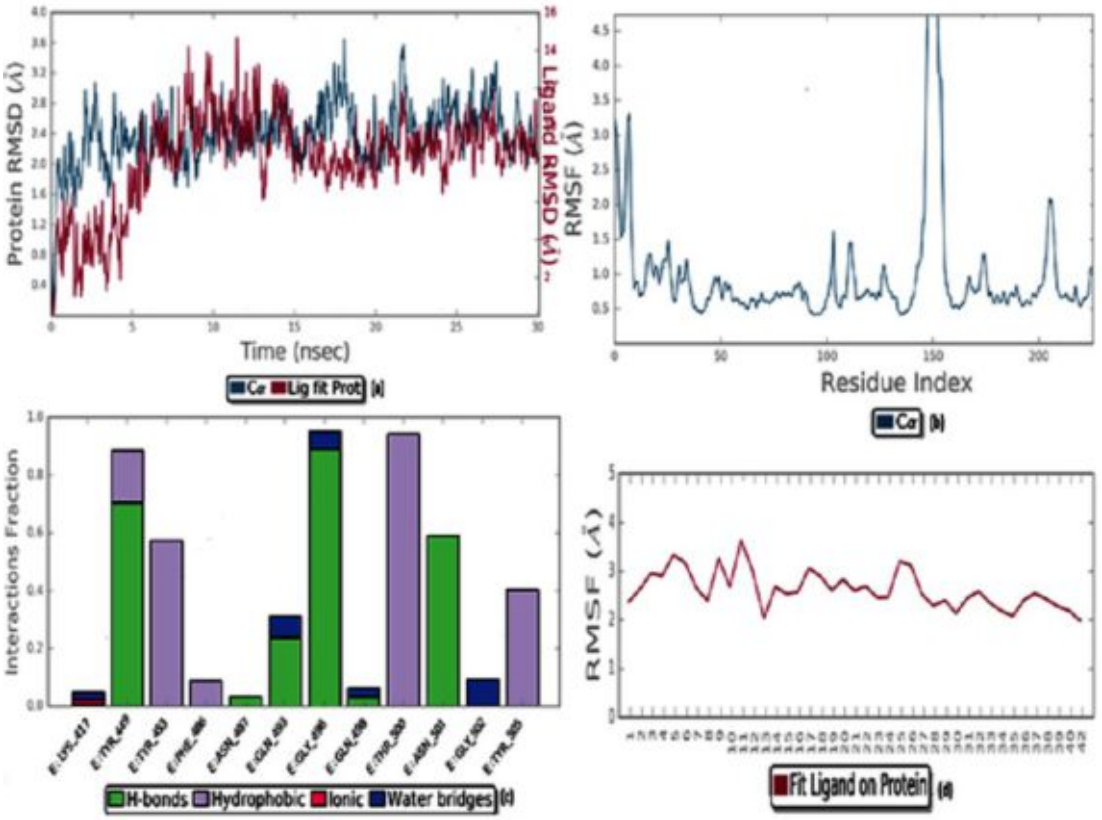

Figure 5. Analysis of MD Simulation Results of 6M0J- ZINC00662497 a) RMSD Plot of 6M0J ZINC00662497 Complex b) RMSF Plot of 6M0J Protein c) RMSF Plot of ZINC00662497 with Respect to 6M0J Protein d) Fraction of Interactions Between 6M0J and ZINC00662497 over the Simulations of 30 ns.

CONCLUSION

In this study, we used combined E-pharmacophore modelling and molecular docking based high throughput virtual screening (HTVS) to identify newer SARS-CoV-2 entry inhibitors. The receptor structure-based pharmacophore model (ADHRR) was developed using the energetic results of docked fragment in to 6M0J protein. Further, the validated pharmacophore hypothesis detailing essential pharmacophoric features was used to screen ZINC and ChEMBL molecular databases to identify potential hits. The resulted 350 hits were further taken for molecular docking based high throughput virtual screening using SARS-Cov-2 entry protein. The retrieved 75 potential hits were again taken for the comparative extra precision (XP) glide docking in to the receptor binding domain of SARS-CoV and SARS-CoV-2. Top 15 promising hits were analysed based on

their fitness scores, docking scores, binding interactions and ADME profiles. The stability of protein-ligand complex and their binding interactions were determined by performing MD simulation of best docked complex for 30ns. Finally, ZINC00662497, ZINC00669387, ZINC08426008, ZINC0660155 and ZINC0844005 were identified as promising leads for the treatment of Covid-19 infections with the highest fitness score and lowest binding free energies. In future, these potential hits will be acquired from vendors and can be used for further in vitro and in vivo studies to evaluate their effectiveness as newer SARS-CoV-2 entry inhibitors and also to validate these combined in silico findings.

CONFLICT OF INTEREST

The authors disclose there is no conflict of interest

ACKNOWLEDGMENT

Authors are thankful to Department of Chemistry, Gujarat University for software facility and Nirma University for providing other necessary facility. Authors gratefully acknowledge the Schrödinger team for resolving technical queries related software.

REFERENCES

1. Liu, Z., Xiao, X., Wei, X., Li, J., Yang, J., Tan, H., Zhu, J., Zhang, Q., Wu, J., and Liu, L. (2020) Composition and divergence of coronavirus spike proteins and host ACE2 receptors predict potential intermediate hosts of SARS CoV 2. *J. Med. Virol.*, **92** (6), 595–601.

2. Lau, S.K.P., Woo, P.C.Y., Li, K.S.M., Huang, Y., Tsoi, H.-W., Wong, B.H.L., Wong, S.S.Y., Leung, S.-Y., Chan, K.-H., and Yuen, K.-Y. (2005) Severe acute respiratory syndrome coronavirus-like virus in Chinese horseshoe bats. *Proc. Natl. Acad. Sci.*, **102** (39), 14040–14045.

3. Guan, Y., Zheng, B.J., He, Y.Q., Liu, X.L., Zhuang, Z.X., Cheung, C.L., Luo, S.W., Li, P.H., Zhang, L.J., and Guan, Y.J. (2003) Isolation and characterization of viruses related to the SARS coronavirus from animals in southern China. *Science (80-.).*, **302** (5643), 276–278.

4. Coutard, B., Valle, C., de Lamballerie, X., Canard, B., Seidah, N.G., and Decroly, E. (2020) The spike glycoprotein of the new coronavirus 2019-nCoV contains a furin-like cleavage site absent in CoV of the same clade. *Antiviral Res.*, **176**, 104742.

5. Huang, C., Wang, Y., Li, X., Ren, L., Zhao, J., Hu, Y., Zhang, L., Fan, G., Xu, J., and Gu, X. (2020) Clinical features of patients infected with 2019 novel coronavirus in Wuhan, China. *Lancet*, **395** (10223), 497–506.

6. Zhao, T.Y., and Patankar, N.A. (2021) Tetracycline as an inhibitor to the SARS-CoV-2. *J. Cell. Biochem.*, **122** (7), 752–759.

7. Wong, S.K., Li, W., Moore, M.J., Choe, H., and Farzan, M. (2004) A 193-amino acid fragment of the SARS coronavirus S protein efficiently binds angiotensin-converting enzyme 2. *J. Biol. Chem.*, **279** (5), 3197–3201.

8. Bhavana, V., Thakor, P., Singh, S.B., and Mehra, N.K. (2020) COVID-19: Pathophysiology, treatment options, nanotechnology approaches, and research agenda to combating the SARS-CoV2 pandemic. *Life Sci.*, **261** (August), 118336.

9. Chan, J.F.-W., Kok, K.-H., Zhu, Z., Chu, H., To, K.K.-W., Yuan, S., and Yuen, K.-Y. (2020) Genomic characterization of the 2019 novel human-pathogenic coronavirus isolated from a patient with atypical pneumonia after visiting Wuhan. *Emerg. Microbes Infect.*, **9** (1), 221–236.

10. Santiesteban-Lores, L.E., Amamura, T.A., da Silva, T.F., Midon, L.M., Carneiro, M.C., Isaac, L., and Bavia, L. (2021) A double edged-sword - The Complement System during SARS-CoV-2 infection. *Life Sci.*, **272** (January), 119245.

11. Colson, P., Rolain, J.-M., Lagier, J.-C., Brouqui, P., and Raoult, D. (2020) Chloroquine and hydroxychloroquine as available weapons to fight COVID-19. *Int J Antimicrob Agents*, **55** (4), 105932.

12. Hoffmann, M., Kleine-Weber, H., Schroeder, S., Krüger, N., Herrler, T., Erichsen, S., Schiergens, T.S., Herrler, G., Wu, N.-H., and Nitsche, A. (2020) SARS-CoV-2 cell entry depends on ACE2 and TMPRSS2 and is blocked by a clinically proven protease inhibitor. *Cell*, **181** (2), 271–280.

13. Costanzo, M., De Giglio, M.A.R., and Roviello, G.N. (2020) SARS-CoV-2: recent reports on antiviral therapies based on lopinavir/ritonavir, darunavir/umifenovir, hydroxychloroquine, remdesivir, favipiravir and other drugs for the treatment of the new coronavirus. *Curr. Med. Chem.*, **27** (27), 4536–4541.

14. Sternberg, A., and Naujokat, C. (2020) Structural features of coronavirus SARS-CoV-2 spike protein: Targets for vaccination. *Life Sci.*, **257** (June), 118056.

15. Verma, K., Lahariya, A.K., Dubey, S., Verma, A.K., Das, A., Schneider, K.A., and Bharti, P.K. (2021) An integrated virtual screening and drug repurposing strategy for the

discovery of new antimalarial drugs against Plasmodium falciparum phosphatidylinositol 3-kinase. *J. Cell. Biochem.*, (February), 1326–1336.

16. Anwar, S., Khan, S., Shamsi, A., Anjum, F., Shafie, A., Islam, A., Ahmad, F., and Hassan, M.I. (2021) Structure-based investigation of MARK4 inhibitory potential of Naringenin for therapeutic management of cancer and neurodegenerative diseases. *J. Cell. Biochem.*, (May), 1445–1459.

17. Lan, J., Ge, J., Yu, J., Shan, S., Zhou, H., Fan, S., Zhang, Q., Shi, X., Wang, Q., and Zhang, L. (2020) Structure of the SARS-CoV-2 spike receptor-binding domain bound to the ACE2 receptor. *Nature*, **581** (7807), 215–220.

18. Liang, J., Pitsillou, E., Karagiannis, C., Darmawan, K.K., Ng, K., Hung, A., and Karagiannis, T.C. (2020) Interaction of the prototypical α-ketoamide inhibitor with the SARS-CoV-2 main protease active site in silico: molecular dynamic simulations highlight the stability of the ligand-protein complex. *Comput. Biol. Chem.*, **87**, 107292.

19. Sterling, T., and Irwin, J.J. (2015) ZINC 15–ligand discovery for everyone. *J. Chem. Inf. Model.*, **55** (11), 2324–2337.

20. Gaulton, A., Bellis, L.J., Bento, A.P., Chambers, J., Davies, M., Hersey, A., Light, Y., McGlinchey, S., Michalovich, D., and Al-Lazikani, B. (2012) ChEMBL: a large-scale bioactivity database for drug discovery. *Nucleic Acids Res.*, **40** (D1), D1100–D1107.

21. Miller III, B.R., and Roitberg, A.E. (2013) Design of e-pharmacophore models using compound fragments for the trans-sialidase of Trypanosoma cruzi: screening for novel inhibitor scaffolds. *J. Mol. Graph. Model.*, **45**, 84–97.

22. Kumar, S., Sharma, P.P., Shankar, U., Kumar, D., Joshi, S.K., Pena, L., Durvasula, R., Kumar, A., Kempaiah, P., and Poonam (2020) Discovery of new hydroxyethylamine analogs against 3CLpro protein target of SARS-CoV-2: Molecular docking, molecular dynamics simulation, and structure–activity relationship studies. *J. Chem. Inf. Model.*

23. Prabhu, S.V., and Singh, S.K. (2019) E-pharmacophore-based screening of mGluR5 negative allosteric modulators for central nervous system disorder. *Comput. Biol. Chem.*, **78**, 414–423.

24. Rohini, K., Agarwal, P., Preethi, B., Shanthi, V., and Ramanathan, K. (2019) Exploring the lead

compounds for Zika Virus NS2B-NS3 protein: an e-pharmacophore-based approach. *Appl. Biochem. Biotechnol.*, **187** (1), 194–210.

25. Joshi, G., Kalra, S., Yadav, U.P., Sharma, P., Singh, P.K., Amrutkar, S., Ansari, A.J., Kumar, S., Sharon, A., and Sharma, S. (2020) E-pharmacophore guided discovery of pyrazolo [1, 5-c] quinazolines as dual inhibitors of topoisomerase-I and histone deacetylase. *Bioorg. Chem.*, **94**, 103409.

26. Damm-Ganamet, K.L., Arora, N., Becart, S., Edwards, J.P., Lebsack, A.D., McAllister, H.M., Nelen, M.I., Rao, N.L., Westover, L., and Wiener, J.J.M. (2019) Accelerating lead identification by high throughput virtual screening: prospective case studies from the pharmaceutical industry. *J. Chem. Inf. Model.*, **59** (5), 2046–2062.

27. Friesner, R.A., Banks, J.L., Murphy, R.B., Halgren, T.A., Klicic, J.J., Mainz, D.T., Repasky, M.P., Knoll, E.H., Shelley, M., and Perry, J.K. (2004) Glide: a new approach for rapid, accurate docking and scoring. 1. Method and assessment of docking accuracy. *J. Med. Chem.*, **47** (7), 1739–1749.

28. Ozgencil, F., Eren, G., Ozkan, Y., Guntekin-Ergun, S., and Cetin-Atalay, R. (2020) Identification of small-molecule urea derivatives as novel NAMPT inhibitors via pharmacophore-based virtual screening. *Bioorg. Med. Chem.*, **28** (1), 115217.

29. Lagarias, P., Barkan, K., Tzortzini, E., Stampelou, M., Vrontaki, E., Ladds, G., and Kolocouris, A. (2019) Insights to the binding of a selective adenosine A3 receptor antagonist using molecular dynamic simulations, MM-PBSA and MM-GBSA free energy calculations, and mutagenesis. *J. Chem. Inf. Model.*, **59** (12), 5183–5197.